SOCIETY OF PETROLEUM ENGINEERS OF AIME

DATA FORM

GL03850

The information that will appear on your paper as it is printed will be taken from this Data Form. PLEASE COMPLETE BOTH SIDES. If you need to discuss your paper, write or call the Proceedings Editor in Dallas, (214) 361-6601. Thank you.

SPE PAPER NUMBER: 6825 MEETING: 52nd SPE Fall Meeting

TITLE: An Analysis of Production from Geopressured Geothermal Aquifers

Please list authors in the order in which they should appear on the paper:

PRIMARY AUTHOR: R.M. Knapp SPE-AIME Member? Yes Citizenship: U.S.

Company affiliation: Petroleum Engineering Dept. Telephone/Telex: (512) 471-5393

Address: The University of Texas, Austin, Texas 78712

CO-AUTHOR: O.F. Isokrari SPE-AIME Member? Yes Citizenship: Nigerian

Company/address: *Petroleum Engineering Dept., The University of Texas, Austin, Tx. 78712

CO-AUTHOR: S.K. Garg SPE-AIME Member? No Citizenship: U.S.

Company/address: Systems, Science and Software, La Jolla, California 92038

CO-AUTHOR: J.W. Pritchett SPE-AIME Member? No Citizenship: U.S.

Company/address: Systems, Science and Software, La Jolla, California 92038

If there are additional authors, please supply names and company affiliations on a separate sheet.

*Current address: AMOCO Production Research, Tulsa, Oklahoma 74102

ORDER FORM FOR PRESS OVERRUNS

*Additional copies of your paper may be ordered when you send in the manuscript at the rate of $15 per 100. You may use the space below as an order form. The minimum order is 100 copies; all orders must be received prior to printing date in order to receive the special rate.**

Number of papers: _____ please give a street address, rather than a box number, for delivery.

Send to: _____

_____

*SPE Fall Meeting authors receive 50 complimentary copies of their paper; regional meeting authors are customarily provided with 25 copies by the sponsoring section.

Please PROOFREAD your paper carefully. It will normally not be possible to make corrections once received by the SPE staff.

You should have included 2 (two) copies of each figure, of high reproducible quality and clearly but lightly numbered on the back. Remember, each table or figure adds 250 words to the length of your paper (with 4 to 5 to a page) and should ideally be capable of legible reduction to a average width of 3 ½ inches. Unusually large figures that require an entire page are equivalent to 1000 words.

FIGURE CAPTIONS should be listed separately listed below in the space provided. Captions must be short and concise. Lengthy discussions of the illustrations should be limited to the body of your paper.

Number of Tables: 1 Number of Figures: 6

Figure Captions

Fig. 1 - Areal view of the hypothetical bounded reservoir.

Fig. 2 - Effects of Solution Gas, Compaction, Shale Water Influx and Reinjection on the Well Block Pressure History

Fig. 3 - Side View of Cross-sectional Reservoir with Adjacent and Underlying Shales

Fig. 4 - Effects of Shale Water Influx on Production Sink Pressure History

Fig. 5 - Areal View of Reservoir Showing Locations of Wells

Fig. 6 - Per Well Production Rate and Cumulative Methane Production Histories of Production Alternatives

Fig. 7 -

Fig. 8 -

Fig. 9 -

Fig. 10 -

Fig. 11 -

Fig. 12 -

If the number of your figures exceeds 12, please continue on a separate sheet.

SPE
Society of Petroleum Engineers of AIME

This paper was presented at the 52nd Annual Fall Technical Conference and Exhibition of the Society of Petroleum Engineers of AIME, held in Denver, Colorado, Oct. 9-12, 1977. The material is subject to correction by the author. Permission to copy is restricted to an abstract of not more than 300 words. Write: 6200 N. Central Expy, Dallas, Texas 75206.

ABSTRACT

The Gulf Coast region of the United States is underlain by deeply buried sandstone reservoirs containing low salinity water at abnormal pressures and elevated temperatures. In addition, the water is believed to contain significant amounts of dissolved natural gas. This geothermal resource, if present in sufficient recoverable quantities, has great energy producing potential and is located in one of the nation's major energy consuming areas. Dorfman and Kehle[1] estimate the energy contained within the geopressured aquifers of Texas may be as much as 20,000 MW centuries excluding the natural gas.

A comprehensive theoretical formulation is presented for the important thermomechanical processes operative in a geopressured geothermal reservoir. The formulation includes the effects of four major drive mechanisms (pore fluid compressibility, reservoir rock compaction, the evolution of dissolved natural gas and the influx of water from adjacent shale formations) expected to be operative during the productive life of the reservoir. Finite difference techniques were used to solve the governing equations describing mass conservation, momentum and energy transport for two flowing phases in a multidimensional heterogeneous reservoir. Constitutive equations were used to describe the changes of fluid properties and reservoir parameters with changes in reservoir pressure and temperature. A series of test calculations were performed to assess the sensitivity of reservoir performance to the gas in solution, sediment compaction and the reinjection of waste fluids. Based on these calculations, it is concluded that sediment compaction and water from interbedded shales can be significant depletion drive mechanisms in geopressured aquifers. The natural gas drive will probably not exceed the water expansion unless there is a significant initial gas saturation. Costs permitting, reinjection of produced fluids into geopressured geothermal aquifers will be desirable to both increase the recovery of thermal energy and natural gas.

References and illustrations at end of paper.

INTRODUCTION

Geothermal energy is presently a small but viable contributor to the United States' energy supply. In addition to known areas of geothermal reserves in the western United States, a unique form of potential geothermal energy exists at moderate to great depths in geopressured aquifers underlying the United States Gulf Coast. Water from such geopressured aquifers often contains natural gas in solution. The geothermal water may be converted into electrical energy after lowering the pressure to extract the natural gas content. Moreover, the fact that temperatures in geothermal reservoirs change very little with time makes geothermal geopressured reservoirs a potentially attractive source of geothermal energy, as there may exist sufficient pressure in these reservoirs to deliver substantial amounts of fluid.

The northern shoreline of the Gulf of Mexico extends more than 1,000 miles,[2] from the Rio Grande River to the Florida panhandle. Underlying a large portion of this shoreline area, both onshore and offshore, in a strip 200 to 300 miles wide are clastic sedimentary deposits of great thickness.

The penetration of sands into underlying muds as a result of continuing deposition or faulting resulted in isolation of large sand members from continuous permeability channels to the overlying strata.[3] Above the intervals thus isolated, pressure throughout the basin approximate 0.465 psi/ft. This is considered normal hydrostatic pressure based on the fluid pressures exerted by a column of saline water. However, beneath the normally pressured zones the isolated units of shales and sands contain pressures far greater than normal. These abnormally pressured zones are now commonly referred to as geopressured zones. Dickey[4] and Dorfman and Kehle[1] state that the generation of geopressure is primarily the result of compaction phenomena. Newly deposited sediments have high porosities and are saturated with water. As they are overlain by younger sediments and buried deeper, the pressure of overburden seeks to reduce the thickness and porosities of these deeper

sediments. As both the rock and water have very low compressibilities, the only way the rock volume can be appreciably reduced is by expelling water, with a consequent decrease in porosity. The rate of expulsion of water is controlled by the permeability of the overlying rocks. If none of the water can escape, then the weight of the overburden causes the fluids contained in the lower sediments to bear a portion of the overburden load. The result is an increase in sediment and fluid pressure. Pressure gradients in the geopressured regions often approach lithostatic pressure, or 1 psi/ft.

Temperature is also important if the heat content of produced water is to be utilized as an energy source. It is apparent from studies of well logs run in boreholes in the Gulf Coast that temperature gradients of approximately 1.5°F/100 ft of depth are found in hydropressured sediments of the Gulf Coast Basin. Gradients in excess of 3°F/100 ft of depth are encountered in geopressured zones. Temperatures at depths of 10,000 feet often range from 225°F to 300°F, and at depths of 15,000 feet it is not uncommon to encounter temperatures in excess of 350°F.

Source beds for most if not all hydrocarbons within the Cenozoic portion of the Gulf Coast Basin are believed to be the shales within the geopressured zones. These beds have provided adjacent sands within the geopressured regions with certain concentrations of natural gas in solution, and great interest has been evidenced in the recovery of appreciable volumes of natural gas from geopressure water. Evidence of natural gas concentration in geopressured zones is based upon information obtained from drilling into geopressured sandstones. Timko[5] found that most of these reservoirs do contain gas in solution. Experimental studies by Culberson and McKetta[6,7] indicate that between 30 and 55 standard cubic feet per barrel of water may be contained in solution in waters under high temperature and pressure encountered in geopressured zones. Buckley, Hocott, and Taggart[8] made extensive investigations into the distribution of hydrocarbons dissolved in waters in the hydropressured regions of the Gulf Coast Basin. Several drill-stem tests on wells in the Frio Formation indicated that the waters were essentially saturated at reservoir conditions. Marsden and Kawai[9] reported on "suiyosei-tennengosu," or natural gas dissolved in brine, found in over a dozen fields throughout Japan. At least two of these fields near Niigata and Tokyo produce gas commercially. Therefore, inferential evidence would indicate that waters in geopressured zones should be essentially saturated with methane.

Water salinity is also a parameter of interest in evaluating the geopressured resources. Empirical evidence, together with laboratory studies by Burst[10] indicates that water salinities within the geopressured zones are considerably lower than those found in normally pressured horizons. Low salinity waters can hold more methane in solution and may have direct usefulness for a variety of process heat or other applications.

Duggan,[11] Wallace,[12] and Harville and Hawkins,[13] gave possible explanations for the difference between volumetric calculations of initial gas in place in geopressured reservoirs and extrapolated p/z (or pressure) data. Some of their explanations were: (a) shale dewatering; (b) change in reservoir compressibility; and (c) other possible sources of water influx. Wallace[12] further advanced the theory of shale dewatering. The idea of changes in rock compressibility and porosity during reservoir depletion was first presented by Hall.[14]

Potential exploitation of geopressured aquifers makes it important to be able to model geopressured geothermal systems so that extraction techniques can be improved, long-term forecasts can be made of performance using various extraction strategies, and potential surface subsidence problems can be identified. One of the most important aspects in developing a reservoir model is the development of comprehensive equations that describe the system.

Several important drive mechanisms in these reservoirs have been identified.[1,15] These mechanisms are (1) reservoir fluid expansion (2) formation compaction, (3) shale water influx, and (4) natural gas dissolved in geothermal waters.

In this paper general balance laws and constitutive relations are developed for geothermal geopressured reservoirs. An interacting rock-fluid system is considered. Typical rock-fluid interactions involve momentum and energy transfer and the dependence of rock porosity and permeability upon fluid pressures and rock stresses. Finite difference techniques were employed to solve the partial differential equations. The relative contributions of the different reservoir mechanisms are presented for three illustrative reservoirs.

PREVIOUS WORK RELATING TO THE DEVELOPMENT OF GEOPRESSURED GEOTHERMAL RESERVOIR SIMULATORS

A number of studies have concentrated on the theoretical analysis of reservoir compaction, which is an important consideration in modeling undercompacted reservoirs. Biot[16] first presented the general theory of three dimensional consolidation. He later[17] developed a theory of elasticity and consolidation for a porous anisotropic solid. Van der Knaap[18] presented an analysis of changes in reservoir volume due to change in pore and overburden pressures. Teeuw[19] concluded that the interpretation of experimental techniques is complicated by the nonlinear compaction behavior of porous rocks. He derived theoretical expressions that interrelate uniaxial and hydrostatic compaction which enables the prediction of in situ reservoir compaction from hydrostatic cell compaction data. Garg and Nur[20] made a detailed study of effective stress laws for fluid-saturated porous rocks. They explored the functional relationship between various definitions of effective stress, i.e., conventional, Biot-Willis-Nur-Byerlee, and theory of interacting continua (TINC). They used stress-strain data on dry and saturated Weber sandstone to demonstrate that the convential effective stress law overestimates the pore pressure effect, whereas the Biot-Willis-Nur-Byerlee and TINC laws underestimate this effect.

Fatt and Davis[21] found that an increase in overburden pressure results in a reduction of absolute permeability. Young et al. (1964) reported a substantial permeability reduction at only 1595 psi effective overburden pressure.

Several studies have been made that are useful

for aiding in the development of a numerical model to simulate geopressured geothermal reservoirs. Raats and Klute[22,23] studied fluid transport in soils and developed mass balance equations and momentum balance equations. Pinder and Bredehoeft[24] described the application of digital computers for aquifer evaluation. Pinder and Frind[25] later used the Galerkin technique to simulate aquifers. Donaldson[26] developed a two-phase one-dimensional geothermal reservoir steady state model, but his model did not simulate production. Whiting and Ramey[27] and Brigham and Morrow[28] developed geothermal models of vapor dominated reservoirs using lumped parameter formulations. Mercer[29] used the finite element approach to simulate the Wairakai, New Zealand, hydrothermal system. He used partial differential equations describing heat momentum transport for a single fluid phase in two dimensions. Finol and Farouq Ali[30] developed two-phase simulators for two-dimensional oil flow in a compacting reservoir, utilizing Geertsma's theory.[31,32] They adapted a rectangular system for predicting ground subsidence. Bourgoyne et al.[33] presented a one-phase, one-dimensional fluid equation used in the study of shale water as a pressure support mechanism.

All the above-mentioned studies are useful in aiding the development of geothermal geopressured models. There is, however, no study known that deals with the numerical simulation of geothermal geopressured reservoirs. Such a model should be able to incorporate all the important reservoir drive mechanisms in geothermal geopressured aquifers such as sediment compressibility, shale water influx, natural gas in solution, and reservoir fluid expansion.

MATHEMATICAL MODEL

A mathematical formulation for modeling a geopressured geothermal reservoir is described in this section. The formulation includes the various phenomena of importance in the behavior of such reservoirs. The resulting governing equations are similar to those for multiphase convective hydrothermal reservoirs except for the presence of the natural gas components (Isokrari,[34] Knapp & Isokrari[15] and Garg et al.[35]).

Balance laws for a rock mixture are written subject to the following assumptions: (1) The fluids and the rock matrix are in local thermal equilibrium (2) The water and free-gas are in local thermal and capillary pressure equilibrium (3) As the pore pressure declines the reservoir compacts in a vertical direction, and (4) Fluid motion is governed by Darcy's Law. The equations expressing mass conservation can be written as follows:

Water Component

$$-\nabla \cdot \left[\rho_w \bar{V}_w\right] + q_w = \frac{\partial}{\partial t}\left[\rho_w \phi S_w\right] \quad \ldots(1)$$

Gas Component

$$-\nabla \cdot \left[\rho_g \bar{V}_g + \rho_w \bar{V}_w R_{sw}\right] + q_g = \frac{\partial}{\partial t}\left[\phi \rho_g S_g + \rho_w S_w R_{sw} \phi\right] \quad \ldots(2)$$

Momentum conservation can be expressed using Darcy's Law for two phase flow.

For the water phase:

$$\bar{V}_w = \frac{-k_{rw}}{\mu_w} k\left[\nabla P_w - \gamma_w \nabla h\right] \quad \ldots(3)$$

For the gas phase:

$$\bar{V}_g = \frac{k_{rg}}{\mu_g} k\left[\nabla P_g - \gamma_g \nabla h\right] \quad \ldots(4)$$

These equations may be combined by substituting equations (3 and 4) in (1 and 2) to give:

$$\nabla \cdot \left[\rho_w \frac{k_{rw}}{\mu_w} k\left[\nabla P_w - \gamma_w \nabla h\right]\right] + q_w = \frac{1}{5.615}\frac{\partial}{\partial t}\left[\rho_w \phi S_w\right] \quad \ldots(5)$$

$$\nabla \cdot \left[\rho_g \frac{k_{rg}}{\mu_g} k\left[\nabla P_g - \gamma_g \nabla h\right]\right] + \nabla \cdot \left[\rho_w \frac{k_{rw}}{\mu_w} R_{sw} k\left[\nabla P_w - \gamma_w \nabla h\right]\right] + q_g = \frac{1}{5.615}\frac{\partial}{\partial t}\left[\phi \rho_g S_g + \rho_w S_w R_{sw}\right] \quad \ldots(6)$$

The accumulation terms of (6) and (7) may be expanded using the chain rule for derivatives to obtain general equations describing the mass conservation of the water component:

$$\nabla \cdot \left[\rho_w \frac{k_{rw}}{\mu_w} k\left[\nabla P_w - \gamma_w \nabla h\right]\right] + q_w = \frac{1}{5.615}\left\{\left[\phi S_w \left[\frac{\partial \rho_w}{\partial P}\right]_T + \rho_w S_w \left[\frac{\partial \phi}{\partial P}\right]_T\right]\frac{\partial P_w}{\partial t} + \phi \rho_w \frac{\partial S_w}{\partial t} + \left[\phi S_w \left[\frac{\partial \rho_w}{\partial T}\right]_P + S_w \rho_w \left[\frac{\partial \phi}{\partial T}\right]_P\right]\frac{\partial T}{\partial t}\right\} \quad \ldots(7)$$

and of the gas component:

$$\nabla \cdot \left[\rho_g \frac{k_{rg} k}{\mu_g} \left(\nabla P_g - \gamma_g \nabla h \right) \right] + \nabla \cdot \left[\rho_w \frac{k_{rw} k}{\mu} R_{sw} \left(\nabla P_w - \gamma_w \nabla h \right) \right] + q_g = \frac{1}{5.615} \left\{ \phi S_g \left(\frac{\partial \rho_g}{\partial P_g} \right)_T \frac{\partial P_g}{\partial t} + \left[\phi S_w R_{sw} \left(\frac{\partial \rho_w}{\partial P_w} \right)_T + \left(\rho_w R_{sw} S_w + \rho_g S_g \right) \left(\frac{\partial \phi}{\partial P_w} \right)_T + \phi \rho_w \left(\frac{\partial R_{sw}}{\partial P_w} \right)_T \right] \frac{\partial P_w}{\partial t} + \phi \rho_g \frac{\partial S_g}{\partial t} + \rho_w R_{sw} \phi \frac{\partial S_w}{\partial t} + \left[\phi \rho_w S_w \left(\frac{\partial R_{sw}}{\partial T} \right)_P + \phi \left[S_w R_{sw} \left(\frac{\partial \rho_w}{\partial T} \right)_P + S_g \left(\frac{\partial \rho_g}{\partial T} \right)_P \right] + \left[R_s \rho_w S_w + \rho_g S_g \right] \left(\frac{\partial \phi}{\partial T} \right)_P \right] \frac{\partial T}{\partial t} \right\} \quad (8)$$

The energy transport equation expressed in terms of temperatures can be written as:

$$\left\langle (1-\phi) \rho_{rm} C_{vrm} + \left[S_g \rho_g C_{vg} + (1+R_{sw}) \rho_w S_w C_{vw} \right] \phi \right\rangle \frac{\partial T}{\partial t} + \left[\left(\phi \rho_w S_w C_{vw} \bar{V}_w \right) + \phi \left(S_g \rho_g C_{vg} \bar{V}_g + S_w \rho_w R_{sw} C_{vw} \bar{V}_w \right) \right] \cdot \nabla T = \nabla \cdot \left[K_m \nabla T \right] + q_w C_{vw} T + q_g C_{vg} T + Q \quad (9)$$

where the pressure work terms have been neglected. The velocities in the energy equation can be determined using equations (3 and 4).

The initial conditions are such that the pressure and temperature in the reservoir must be specified. The reservoir distribution of all secondary dependent variables can be calculated from these. Independent parameters defining the aquifer are specified for the sand sediment and for the adjacent shales. For cross-sectional studies the reservoir is initially assumed to be in hydrostatic and thermal equilibrium.

The momentum transport boundary conditions used are no-flow boundary conditions for both water and gas phases. The boundary conditions for the heat transport equation can vary. For the studies described later, no heat transport across the boundaries was allowed. This is a very conservative assumption.

A model has been developed where the properties of rock and/or fluid are allowed to vary in space as well as time. The resulting problem can only be solved numerically with the aid of a computer.

Constitutive Relations for the Pore Fluid

The difference in gas and water phase pressures is the capillary pressure.

$$P_c = P_g - P_w \quad (10)$$

The phase saturations sum to one.

$$S_w + S_g = 1.0 \quad (11)$$

The water component in geopressured reservoirs is expected to remain in the liquid state. The density of fresh water can be estimated using data from the ASME Steam Tables.[36] This can be corrected for total dissolved solids using the correlation of Brill and Beggs[37] and for the gas dissolved in the water using the Dodson and Standing[38] correlations extended into the geopressured regions.[37]

Natural gases found in geopressured reservoirs have very high methane content. Therefore, gas deviation factors for methane were used with the real gas law to estimate gas density.

Data on the viscosity of impure water are meager. Water viscosity should generally increase with increases in pressure and dissolved solids and should decrease with increases in temperature and gas in solution. Data on the effects of gas in solution on the viscosity of water are not available at this time. However, the effect of temperature on the viscosity of water was reported by Ramey et al.[39] and Van Wingen.[40] An expression which can be used to approximate an average curve for Van Wingen's data is provided by Brill and Beggs[37] as:

$$\mu_w = \text{EXP}\left(1.003 - 1.479 \times 10^{-2} + 1.983 \times 10^{-5} T^{-2}\right) \quad (12)$$

where T is in °F.

Van Wingen's data on the viscosity of oil field brines at pressures to 7100 psia and temperatures to 300°F suggest that dissolved solids (up to 60,000 ppm) have only a small effect on the viscosity of saline brines.

The viscosity of gases under pressure can be estimated using the correlation by Lee et al.[41]

The Lee et al. correlation consists of a series of equations as follows:

$$\mu_g = K \cdot 10^{-4} \text{EXP}(X \rho^y) \quad (13)$$

where

$$K = \frac{(9.4 + 0.02M) T^{1.5}}{209 + 19M + T}$$

$$X = 3.5 + \frac{986}{T} + 0.01M$$

$$y = 2.4 - 0.2X$$

and

M = molecular weight

T = temperature, °R

Under conditions of increasing pressure, water will absorb available gas into solution. Experimental studies by Culberson and McKetta[6,7] indicate that

between 30 and 55 scf/bbl of water may be contained in solution in waters under the high temperatures and pressures encountered in geopressured zones. Although others, Brill and Beggs,[37] Amarijafari and Campbell,[42] and Dodson and Standing,[38] have studied gas solubility in water, their investigations do not extend into the temperature and pressure ranges expected in geopressured aquifers. Therefore, it is probably best to accept the Culberson and McKetta data on methane solubility in studies of geopressured reservoirs at this time.

The study by Dodson and Standing[38] also investigated solubility of the natural gas in two brines at a temperature range of 100° to 200°F. The concentrations of the two brines were 8,630 ppm and 34,100 ppm to dissolved solids respectively. They proposed a linear correction factor to solubility in fresh water. A more detailed graph of the linear correction factor is given by Brill and Beggs[37] and has been used to correct for gas solubility in this study.

Constitutive Relations for the Rock Matrix

Several functions for the rock matrix need to be prescribed.

Porosity is a function of position, the state of stress and temperature. If it is assumed that (1) the reservoir compaction is uniaxial and (2) the overburden remains essentially constant, then it can be shown that incremental changes in porosity are given by the following expression(Knapp and Isokrari[15] and Garg et al.[35]):

$$\frac{\partial \phi}{\partial t} = (1-\phi)\left\{C_m \frac{\partial P}{\partial t} + \left[C_T - 3\eta_s\right] \frac{\partial T}{\partial t}\right\}$$

where

$$C_m = \frac{1}{K + 4/3\,\mu_p}$$

$$C_T = \frac{3\eta K}{K + 4/3\,\mu_p} \quad \ldots\ldots\ldots\ldots (14)$$

In the above relationship for ϕ, it is implicitly assumed that the bulk modulus of the porous rock K is much smaller than the bulk modulus of the rock grain K_s ($K \ll K_s$).

The rock permeability k is a complex function of the rock and fluid stresses as well as temperature (Brace,[43] Ramey, et al.[39]). It is often postulated that this dependence is primarily exhibited through changes in porosity . There exist in the literature numerous empirical expressions relating k to . In the present study, we will employ the empirical expression:

$$k = k_0 \ \text{EXP}\left[\frac{\phi - \phi_0}{(1-\phi_0)(1-\phi)}\right] \quad \ldots\ldots (15)$$

where k_0 is the permeability corresponding to the initial porosity ϕ_0.

At the present time, sufficient data are not available to determine the dependence of relative permeabilities on temperature; it will be, therefore, assumed that the relative permeabilities are functions only of saturation. In particular, the relative permeabilities may be represented by the equations of Corey, et al.:[44]

$$k_{rw} = (S_w^*)^4$$

$$K_{rg} = (1-S_w^*)^2$$

where

$$S_w^* = (S_w - S_{wr})/(1 - S_{wr} - S_{gr})$$

$$S_w = 1 - S_g \quad \ldots\ldots\ldots\ldots (16)$$

Here S_{wr} (S_{gr}) is irreducible water (gas) saturation, and S_w^* is the volumetric liquid saturation normalized with respect to the mobile fluid saturation in the pore space.

Ramey, et al.[39] present a review of the measurements and empirical formulae for the thermal conductivity of dry and fluid-saturated rocks. The thermal conductivity of most rocks decreases with an increase in temperature. Thermal conductivities of fluid-saturated rocks are two to five times greater than those of dry rocks; this result suggests that the rule of mixtures formula is not generally valid. In the absence of detailed experimental data, $\dot{K}_m$ may be adequately approximated by the following relationship due to Budiansky:[45]

$$(1-\phi)\left[\frac{2}{3} + \frac{1}{3}\frac{\dot{K}_{rm}}{\dot{K}_m}\right]^{-1} + \phi\left\{(1-S)\left[\frac{2}{3} + \frac{1}{3}\frac{\dot{K}_w}{\dot{K}_m}\right]^{-1} + S\left[\frac{2}{3} + \frac{1}{3}\frac{\dot{K}_g}{\dot{K}_m}\right]^{-1}\right\} = 1. \quad \ldots\ldots\ldots (17)$$

The formation compaction may be calculated by multiplying the strain caused by production by the reservoir thickness, Geertsma[32] and Isokrari:[34]

$$\frac{\partial \Delta Z}{\partial t} = L_z\left[C_m \frac{\partial P_w}{\partial t} + C_T \frac{\partial T}{\partial t}\right] \quad \ldots\ldots (18)$$

Numerical Solution

The partial differential equations describing component and energy transport (Eqs. 7 , 8 and 9) were solved using the finite difference method. Central difference approximations were used to represent the spatial derivatives and backward differences were used to represent the time derivatives. Interblock fluid properties were evaluated as arithmetic averages. Formation parameters such as thickness and permeability were evaluated using series weighting. Relative permeabilities and advection terms were determined by upstream weighting.

The algebraic equations resulting from the finite difference approximations of the flow equations (7 and 8) were solved using the line successive over-relaxation technique (LSOR) described by Watts[46] and Young and Gregory.[47] When these equations are written for each point on a line, they produce a bi-tridiagonal matrix which can be solved using the algorithm of Douglas, et al.[48] This approach allows phase

pressures to be calculated directly. The phase pressures can then be used to evaluate pressure dependent terms as necessary. The program was written so that both implicit or explicit mobility techniques can be used depending on the problem to be solved. LSOR is also used to solve the energy transport equation. Variable grid block sizes and heterogeneous reservoir properties may be used in any particular problem. Material and energy balances were used as checks of the computational accuracy of the program.

The solution procedures employed are well known and details are given in Reference 34.

RESERVOIR SIMULATION STUDIES

In this section, a series of calculations designed to assess the effects of gas drive, reservoir compaction, shale water influx and fluid reinjection on reservoir behavior are presented. Three conceptual reservoirs were studied. The first reservoir approximates a prospective geothermal geopressured reservoir. The second reservoir is a cross-sectional study which demonstrates the effects of shale water influx and the third reservoir compares two different production strategies for the first reservoir.

Consider a representative hypothetical bounded (no mass or energy flux across the boundaries) geopressured reserovir. The reservoir consists of a rectangular cube with the following dimensions: Length = 51,865 ft, Width = 23,650 ft, Thickness = 162 ft, Depth = 13,000 ft. The reason for the unusual choice of reserovir dimensions is that they approximate the reservoir volume of a prospective aquifer in Kenedy County, Texas. A two-dimensional areal representation of the reservoir is shown in Figure 1. An 11 x 9 grid was used to represent the sandstone part of the reservoir (11 x 13 if the shale sediments were included). The initial reservoir fluid temperature and pressure are assumed to be 300°F and 11,000 psia, respectively. Since the studies reported are for an areal configuration, the entire reservoir fluid is taken to be initially at a uniform pressure and temperature. The reservoir rock is assumed to have the properties given in Table 1.

In the studies described below, a single well located at the center of the reservoir (block 5, 6) was produced at a constant rate of 40,000 bbl/day. For the purposes of simulation, production was continued for 30 years or until the well-block pressure fell below 5,000 psia.

Run 1 is the base case for these analyses. This run used only the energy contained in the compressed pure water. For subsequent runs other sources of reservoir energy were added. With only water expansion as a source of energy the reservoir was depleted in about 8 years. Figure 2, Run 1 shows the well block pressure generated in this study. Within 1 year the well seems to be on volumetric depletion.

Run 2 added the effect of dissolved natural gas. The water was assumed to be saturated with natural gas. As the pressure declines during production, natural gas evolves during production. The maximum gas saturation in the well block at the end of 11 years is approximately 2 percent. The principal effect of the natural gas is to extend the reservoir's productive life as shown in Figure 2.

Because geopressured geothermal reservoirs are undercompacted, these reservoirs are subjected to compaction as the reservoirs are depleted. This formation compaction can be a significant source of energy. To account for this source of energy, a uniaxial compaction coefficient of 12.1×10^{-6} psi^{-1} was used. Thus, Run 3 of Figure 2 accounts for the reservoir water expansion of Run 1 as well as the effect of formation compaction. Notice that the wellbore block pressure does not drop below 9,000 psi during the 30 year producing life.

For Run 4, a "band" of shale was placed offshore (see Figure 1). Shale permeability was estimated to be 10^{-4} md and the shale sediment compressibility was increased to 8.7×10^{-5} psia. This is a seven fold increase over sandstone compressibility. The porosity used was the same as the sandstone (0.216). The well position was unchanged. The well block pressure generated in Run 4 is shown on Figure 2 and is slightly higher than that generated in Run 3. A comparison of the curves shows that it would be difficult to distinguish effect of offshore shale water influx compared to sediment compaction. Even though the volume of shale added to the simulated aquifer is small, it was apparently adequate for the simulation because the pressure at the outside boundary of the shale had not decreased from the initial pressure even after 30 years of production. In fact, most of the shale water influx has come from the first half mile of the shale.

In Runs 1, 3 and 4 it was assumed that the reservoir contains no gas dissolved in the geothermal waters. Run 2 provides a demonstration of the drive effectiveness of the dissolved natural gas. Run 5 includes the effects of all potential sources of reservoir drives for this particular reservoir. The well block pressure generated is shown as Run 5 in Figure 2. The maximum free gas saturation is approximately 1 per cent. A comparison of Runs 4 and 5 shows that the pressures of Run 5 are consistently but only slightly higher than those of Run 4.

An inspection of Figure 2 shows that the most important source of reservoir energy is sediment compressibility. The effect of shale water influx does not appear to be quite clear and needs to be examined in greater detail since the most effective sources of shale water would be expected to be shales interbedded with the sandstone and those located below the sandstone.

From Figure 2, it can be seen that only in the case of water expansion is the early transient behavior exceeded in less than 1 year. For the other cases it would take 5 to 10 years to establish semi-steady state decline. Therefore, it will be difficult to obtain information on reservoir limits from a short-term drawdown test in a system this large. To discern drive contribution of the different sources it will be necessary to make all possible efforts to obtain independent estimates of reservoir parameters from sources of data other than well tests.

In the five cases above, Run 1 was subjected to the highest pressure drawdown. Therefore, Run 1 was used to examine the behavior of formation temperature under the assumption of no thermal energy gain from adjacent formations. The maxiumum temperature decrease was 1.5°F and the pressure response is

indistinguishable from Run 1.

Reinjection has been recoginzed by several authors (see e.g., Garg,et al.[49] and Pritchett, et al.[50,51]) as being highly desirable for (1) efficiently extracting heat energy from a geothermal reservoir, (2) disposing of large volumes of produced fluids, and (3) preventing ground surface subsidence. In Run 6 (otherwise identical with Run 2), approximately half of the produced water was reinjected into the reservoir. The geometry of the reinjection system is shown in Figure 1; the reinjected fluid was pure water at approximately 77°F. It can be seen from Figure 2 that reinjection (even in the absence of sediment compaction) can be used to significantly extend the useful life and production of the reservoir. Reinjection tends to raise pore pressures and to lower gas saturations in the reservoir.

A second, cross-sectional, reservoir was studied to further investigate the effects of water influx from adjacent and underlying shales. The reservoir used has a length and width of 5200 feet respectively and a thickness of 300 feet. The base case has similar reservoir properties to Run 3 of the first reservoir except that gravity was considered in this case; thus pressure varies through the thickness of the reservoir. The initial reservoir pressure was 11,000 psi at the midpoint of the formation and the reservoir temperature was held at 300°F for all cross sectional runs. The initial absolute permeability of the sandstone was estimated to be 2.5 md. The production line sink was located 1,418 ft from the sand-shale boundary and produced 40,000 B/D from throughout the sandstone formation. For the base case no water influx from shale was allowed. The average sink block pressure as a function of time is shown in Figure 4 as Run 7.

To examine the effect of offshore shale water influx a "band" of 2,836 ft of shale was added to the edge of the reservoir (see Figure 3). The horizontal and vertical shale permeabilities was estimated as 10^{-4} md and 10^{-5} md respectively. The sink block pressure history generated is given in Figure 4 as Run 8. The curve generated was consistently higher than the curve of Run 7 and edge water shale could be assumed to be a significant source of reservoir energy.

The next run was made by eliminating the offshore shale and considering only 240 ft of underlying shale. Shale properties were the same as Run 8. The resulting pressure curve is shown in Figure 4 as Run 9. Run 9 shows that water from underlying (or interbedded shales) would be a more effective source of reservoir energy than shales at the edge of the reservoir. When the effects of both underlying and offshore shales were considered the resulting decline curve, Run 10, showed shale water from both sources could provide substantial reservoir energy for production.

A decline curve was then generated that considers gas in solution with simultaneous water influx from underlying and adjacent shales, (Run 11). The effect of the solution gas drive,while recognizable, is not large.

The temporal characteristics of the simulated responses due to shale water influx are the same as those due to expansion of the reservoir fluids and sediment compressibility. Further, the effects of offshore shale water influx could be easily confused with those of underlying shale water influx. It would therefore not be possible to discriminate between these effects from well tests alone.

A HYPOTHETICAL PRODUCTION STRATEGY

The geopressured reservoir geometry studied was very similar to the first reservoir described: the thickness was the same but both the length and width were reduced slightly for convenience. The rock properties considered were essentially the same as in the preceding problems except that:

C_m (sediment compressibility on loading)

$= 12.1 \times 10^{-6}$ psi^{-1}

C_m^U (sediment compressibility on unloading)

$= 4.0 \times 10^{-6}$ psi^{-1}

S_{wr} (residual liquid saturation) = 0.3

S_{gr} (residual gas saturation) = 0.05

Note that rock compaction depends upon the loading direction so that porosity depends, in general, on P, T and the sign of $\frac{\partial P}{\partial t}$.

The fluid within the pores was taken to be at the same pressure (11,000 psi) and temperature (300°F) everywhere within the reservoir initially. The system is also super-saturated with methane, with a uniform initial gas saturation of 5 percent. This free gas is immobile initially, since $S_{gr} = 0.05$ for these runs.

In the preceding problems, the reservoir was penetrated by a single well. Clearly, a large number of wells will be required for efficient exploitation of a reservoir of this size. Accordingly, the line drive well-placement layout illustrated in Figure 5 was adopted for study. This well arrangement consists of an array of 56 production wells, 49 "high-rate" injection wells and 14 "low-rate" injection wells, for a total of 119 wells with 3,220 feet well separation. The "low-rate" injection wells inject fluid at exactly half the rate of the "high-rate" wells. Owing to symmetry, the small rectangular region outlined in Figure 5 by a dotted line is representative of all such elements in the reservoir. This region was simulated with a 7 x 14 grid with an equal grid spacing of 230 ft in each areal direction.

Injection wells were treated as constant flow-rate wells, and injected pure (methane-free) water at a temperature of 77°F. Two cases were considered--one in which the injection rate was taken as zero, and the other in which the injection rate was 22,000 B/D per "high-rate" well. The production wells, on the other hand, were treated as pressure-dependent. For the present runs, the flow rate per well was taken as linearly dependent on the pore pressure in the sink zone, equal to 40,000 STB/day at the initial pressure of 11,000 psi but declining to zero as the pressure reaches the hydrostatic value of 5,100 psi.

The calculations indicated a dramatic difference in the behavior of the system between the no-injection cases, as might be expected. Generally, the results indicate enormously improved reservoir performance if injection is practiced. The no-injection case was simulated to a point corresponding to 11.6 years. At this time, fluid production rates had dropped to 1,325 B/D per well. The injection case was run much longer, to about 56 years.

Total flow rates per production well are shown, as functions of time, in Figure 6 for the two cases. As noted above, without injection the flow rate drops monotonically toward zero. Without the compaction drive, the lifetime of the system would have been even shorter. With injection, on the other hand, flow rates start at 40,000 bbl/day, drop to a minimum at about 20 years, and then slowly increase toward 22,000 bbl/day at late times. Production rates of the natural gas also drop off rapidly toward zero without injection. With injection, natural gas production is maintained much longer but does eventually decline. The differences between the two techniques as regards natural gas production are shown dramatically in Figure 6, which illustrates the cumulative production of methane as a function of time, expressed as a percentage of the total methane initially present in the reservoir. Without injection, less than 10 percent of the methane can be recovered. With injection, it seems clear that over 90 percent can be extracted, even with the relatively simple well-pattern used.

The temperature of the produced fluid is an important factor if the water is to be used for geothermal applications. In the no-injection case, of course, temperatures remain essentially constant. With injection, temperature remains constant for 14 years followed by a steady decline. The temperature of the produced fluid falls below 212°F (100°C) at about 49 years.

The results of this pair of calculations would seem to make a strong case for reinjection into geopressured aquifers as production technique. Even though cold water breakthrough does eventually occur, the lifetime of the field is enormously prolonged. Even if the fluid's heat is considered useless below 140°C (285°F, approximately 26 years production), the injection technique provides 5-1/2 times as much useful fluid as no injection. If the temperature cutoff is 100°C (212°F, approximately 49 years of production), injection produces almost ten times more fluid than no injection. Also, as was seen earlier, over ten times as much methane is recovered if injection is practiced. It would therefore seem desirable to inject fluid into geopressured strata as a method of maintaining and stimulating production.

Obstacles to reinjection into geopressured aquifers are the necessities of building the reinjection network and of supplying power to the injection pumps. An accurate comparison of the "energy cost" of reinjection compared to the "energy benefit" associated with the improved reservoir performance depends strongly upon the details of the surface equipment and is therefore beyond the scope of this study. Reinjection clearly would be more advantageous as the permeability of the prospect increases, since pumping pressures required to maintain a given flow rate in the system decline with increasing permeability. If good reservoir permeability is present, production strategies involving reinjection may prove advantageous.

CONCLUSIONS

On the basis of our study and the simulations conducted the following conclusions are derived.

1. Multiphase fluid flow equations and constitutive relationships describing deformable, anisotropic, heterogeneous, and nonisothermal reservoirs such as the Gulf Coast geopressured goethermal aquifers have been presented. This mathematical model has been numerically solved using a computer program. The major drive mechansims considered include fluid and sediment compressibilities, shale water influx and natural gas in solution. Gravity, capillarity, and pressure and temperature dependence of fluid densities, viscosities and natural gas solubility in water were also considered.
2. It was found that sediment compressibility will be important depletion drive mechanisms in geopressured reservoirs.
3. Based on the shale properties used and assuming static geopressured reservoirs, water influx from adjacent offshore shales into geopressured reservoirs during production occurs mostly from the shales immediately adjacent to the sand-shale interface.
4. Water influx into geopressured reservoirs from underlying or interbedded shales will be more significant than influx from adjacent offshore shales.
5. The effect of initially dissolved gas as a reservoir drive mechanism in geothermal geopressured reservoirs probably will not exceed that of the compressibility of the reservoir fluid.
6. The depletion of geothermal geopressured reservoirs may be regarded as an isothermal process.
7. Costs permitting, reinjection of produced fluids into geopressured geothermal aquifers will be desirable to both increase the recovery of thermal energy and natural gas.

NOMENCLATURE

C_m	Uniaxial compaction coefficient, $psia^{-1}$
C_T	Coefficient of thermal expansion, 1/°F
C_v	Specific heat, Btu/lb°F
h	Depth below a reference datum, ft
K	Bulk modulus of rock, psi
k	Absolute permeability, tensor, Darcy x 1.127
k_r	Relative permeability fraction
L_x	Reservoir length, ft
L_z	Reservoir width (for horizontal studies), ft Reservoir thickness (for vertical studies), ft
M	Molecular weight
P	Pressure, psia
P_c	Capillary pressure, psia

q	Fluid production rate, positive for injection, B/D-cu ft
Q	Heat source strength, Btu/D-cu ft
R_{sw}	Gas solubility in water, scf/STB
S_w	Phase saturation, fraction
t	Time, days
T	Temperature, °F
$\bar{V}$	Macroscopic velocity, B/D-sq ft of area
W	Reservoir width (for vertical studies), ft thickness (for horizontal studies), ft

Greek

γ	Specific weight ($\rho g/144 g_c$), psi/ft
$\Delta\bar{z}$	Reduction in reservoir thickness, ft
η	Coefficient of linear thermal expansion of porous rock, 1/°F
η_s	Coefficient of linear thermal expansion of rock grain, 1/°F
$\dot{\kappa}$	Thermal conductivity, Btu/D-ft°F
μ	Viscosity, cp
μ_p	Rock shear modulus, psi
ρ	Density, lb/cu ft
ϕ	Fractional porosity

Subscripts

o	Initial Conditions
f	Fluid
g	Gas
m	Mixture (rock, water and gas)
rm	Rock matrix
w	Water (wetting phase)
x	In x direction
z	In z direction

ACKNOWLEDGEMENT

This research has been supported by the U.S. Energy Research and Development Administration Contract E(40-1) - 5040 and a grant from the Center for Energy Studies, The University of Texas at Austin. Their financial support is gratefully acknowledged by the authors.

REFERENCES

1. Dorfman, M. and Kehle, R.O. Potential Geothermal Resources of Texas, Geological Circular 74-4, Bureau of Economic Geology, The University of Texas at Austin, 1974.

2. Dorfman, Myron, and Deller, R.W. Summary of Future Projections of Geopressured Geothermal Energy, Vol 1 of Proceedings, Second Geopressured Geothermal Energy Conference, Center for Energy Studies, The University of Texas at Austin, 1976.

3. Dickinson, G. "Geological Aspects of Abnormal Reservoir Pressure in Gulf Coast Louisiana," Bulletin AAPG (1953) 387, no. 2, 410.

4. Dickey, P.A. "Abnormal Pressures in Deep Wells in South Louisiana," Science (1968) 160, no. 3828, 609-615.

5. Timko, D.J. and Fertl, W.H. "Relationship Between Hydrocarbon Accumulation and Geopressure and its Economic Significance," Journal of Petroleum Technology (August 1971), 923.

6. Culberson, O.L. and McKetta, J.J., Jr. "Phase Equilibria in Hydrocarbon-Water Systems III--The Solubility of Methane in Water at Pressures to 10,000 psi," Petroleum Transactions, AIME (1951) 192, 223-226.

7. Culberson, O.L. and McKetta, J.J., Jr. "Phase Equilibria in Hydrocarbon Water Systems IV Vapor-Liquid Equilibrium Constants in the Methane-Water and Ethane-Water Systems," Petroleum Transactions, AIME (1951) 192, 297-300.

8. Buckley, S.E., Hocott, C.R., and Taggart, M.S. "Distribution of Dissolved Hydrocarbons in Subsurface Waters," Habitat of Oil, Louis Weeks Symposium, AAPG (1958), 850-882.

9. Mardsden and Kawai, "Sinyosei-Ten' Nengasu," American Association of Petroleum Geologists Bulletin (1965) 49, no. 3, 286-295.

10. Burst, J.F. "Diagenesis of Gulf Coast Clayey Sediments and Its Possible Relation to Petroleum Migration," AAPG Bulletin (1969) 53, no. 1, 73-93.

11. Duggan, J.O. "The Anderson 'L' - An Abnormally Pressured Gas Reservoir in South Texas," Journal of Petroleum Technology (February 1972) 132.

12. Wallace, W.E. "Water Production from Abnormally Pressured Gas Reservoirs in South Louisiana," Journal of Petroleum Technology (August 1969), 969.

13. Harville, D.W. and Hawkins, M.F. "Rock Compressibility and Failure as Reservoir Mechanisms in Geopressured Gas Reservoirs," Journal of Petroleum Technology (December 1969), 1528.

14. Hall, H.N. "Compressibility of Reservoir Rocks," Transactions AIME, (1953) 198, 309-311.

15. Knapp, R.M. and Isokrari, O.F. "Aspects of Numerical Simulation of Future Performance of Geopressured Geothermal Reservoirs." Proceedings,

Second Geopressured Geothermal Energy Conference, The University of Texas, Austin, Texas (1976) III, 103-161.

16. Biot, M.A. "General Theory of Three Dimensional Consolidation," Journal of Applied Physics, (February 1941) 12, 155-164.

17. Biot, M.A. "Theory of Elasticity and Consolidation for a Porous Anisotropic Solid," Journal of Applied Physics, (1955) 26, 182-185.

18. Van der Knaap, W. "Nonlinear Behavior of Elastic Porous Media," Transactions AIME (1959) 216, 187-197.

19. Teeuw, D. "Prediction of Formation Compaction from Laboratory Compressibility Data," Society of Petroleum Engineering Journal (September 1971) 263-271.

20. Garg, S.K. and Nur, A. "Effective Stress Laws for Fluid-Satruated Prous Rocks," Journal of Geophysical Research (1973) 78, No. 26, 5911.

21. Fatt, I. and Davis, D.H. "The Reduction in Permeability with Overburden Pressure," Transactions, AIME (1952) 195, 329.

22. Raats, P.A.C. and Klute "Transport in Soils: The Balance of Mass," Soil Science Society of America Proceedings (1968) 32, no. 2, 161-166.

23. Raats, P.A.C. and Klute "Transport in Soils: The Balance of Momentum," Soil Science Society of America Proceedings (1968) 32, no. 4, 452-456.

24. Pinder, G.F. and Bredehoeft, J.D. "Application of the Digital Computer for Aquifer Evaluation," Water Resources Research (1968) 4, no. 5, 1069-1093.

25. Pinder, G.F. and Frind, E.O. "Application of Galerkin's Procedure to Aquifer Analysis," Water Resources Research (1972) 8, no. 1, 108-120.

26. Donaldson, I.G. "A Possible Model for Hydrothermal Systems and Methods of Studying Such a Model," Paper 2580 presented at the Third Australaian Conference on Hydraulics and Fluid Mechanics, Sidney Australia, Nov. 25-29, 1968.

27. Whiting, R.L. and Ramey, H.J. "Application of Material and Energy Balances of Geothermal Steam Production," Journal of Petroleum Technology (1969) 21, 893-900.

28. Brigham, W.E. and Morrow, W.B. "P/Z Behavior for Geothermal Steam Reservoirs," paper SPE 4899 presented at the SPE-AIME 44th Annual California Regional Meeting, San Francisco, April 4-5, 1974.

29. Mercer, J.W. Finite Element Approach to the Modelling of Hydrothermal Systems, Ph.D. Thesis, University of Illinois, 1973.

30. Finol, A. and Farouq Ali, S.M. "Numerical Simulation of Oil Production with Simultaneous Ground Subsidence," SPE Journal (October 1975) 15, no. 5, 411-424.

31. Geertsma, J. "The Effect of Fluid Pressure Decline on Volumetric Changes of Porous Rocks," Transactions AIME (1957) 210, 331.

32. Geertsma, J. "Land Subsidence above Compacting Oil and Gas Reservoirs," Journal of Petroleum Technology (June 1973), 734-744.

33. Bourgoyne, A.J., Hawkins, M.F., Laraquinal, F.P. and Wickenhausen, T.L. "Shale Water as a Pressure Mechanism in Superpressure Reservoirs," SPE 3851, presented at the Abnormal Subsurface Pore Pressure Meeting, Baton Rouge, Lousiana, 1972.

34. Isokrari, O.F. Numerical Simulation of United States Gulf Coast Geopressured Geothermal Reservoirs, Ph.D. Thesis, The University of Texas, 1976.

35. Garg, S.K., Pritchett, J.W., Rice, M.H. and Riney, T.D. U.S. Gulf Coast Geopressured Geothermal Reservoir Simulation, Systems, Science and Software Report SS-R-77-3147, February 1977.

36. ASME Steam Tables, Second Ed., The American Society of Mechanical Engineers, New York, 1967.

37. Brill, J.P. and Beggs, H.D. Two Phase Flow in Pipe, University of Tulsa, Oklahoma, 1975.

38. Dodson, C.R. and Standing, M.B. "Pressure-Volume-Temperature and Solubility Relations for Natural Gas-Water Mixtures," Presented at the Spring Meeting, Pacific Coast District Division of Production, Los Angeles, California, March 23, 1944.

39. Ramey, H.J., Jr., W.F. Brigham, H.K. Chen, P.G. Atkinson, and N. Arihara. "Thermodynamic and Hydrodynamic Properties of Hydrothermal Systems," Geothermal Program Report SGP-TR-6, Stanford University, Palo Alto, California, 1974.

40. Van Wingen. Secondary Recovery of Oil in the United States, American Petroleum Institute (1950), 127.

41. Lee, A.L., Gonzales, M.H. and Eakin, B.E. "The Viscosity of Natural Gases," Transactions AIME (1966), 997.

42. Amirijafari, B. and Campbell, J.M. "Solubility of Gaseous Hydrocarbon Mixtures in Water," Transactions, AIME (1972), 21-27.

43. Brace, W.F. "Pore Pressure in Geophysics," in Flow and Fracture of Rocks, American Geophysical Union, Washington, D.C. (1972), 265.

44. Corey, A.T., Rathjens, C.H., Henderson, J.H. and Wyllie, M.J. "Three-Phase Relative Permeability," Transactions AIME, (1956), 207, 349.

45. Budiansky, B. "Thermal and Thermoelastic Properties of Isotropic Composites," J. of

Composite Materials (1970), 4, 286.

46. Watts, J.W. "An Iteratuve Matrix Solution Method Suitable for Anisotropic Problems," Transactions AIME (1971) 251, 47-51.

47. Young, D.M. and Gregory, R.T. A Survey of Numerical Mathematics, Addison Wesley Publishing Company, Reading, Massachusetts, 1973.

48. Douglas, J., Peaceman, D.W., and Rachford, H.H., Jr. "A Method of Calculating Multidimensional Immiscible Displacement," Transactions, AIME (1959) 216, 297-306.

49. Garg, S.K., Brownell, D.H., Jr., Pritchett, J.W. and Herrmann, R.G. "Shock-Wave Propagation in Fluid-Saturated Porous Media," Journal of Applied Physics, (1975), 46, 702.

50. Pritchett, J.W., Garg, S.K., Brownell, D.H., Jr., and Levine, H.B. "Geohydrological Environmental Effects of Geothermal Power Production, Phase I," Systems, Science and Software Report SSS-R-75-2733, 1975.

51. Pritchett, J.W., Garg, S.K., Brownell, D.H., Jr., Rice, L.F., Rice, M.H., Riney, T.D., and Hendrickson, R.R. "Geohydrological Environmental Effects of Geothermal Power Production, Phase II-A," Systems, Science and Software Report SSS-R-77-2998, 1976.

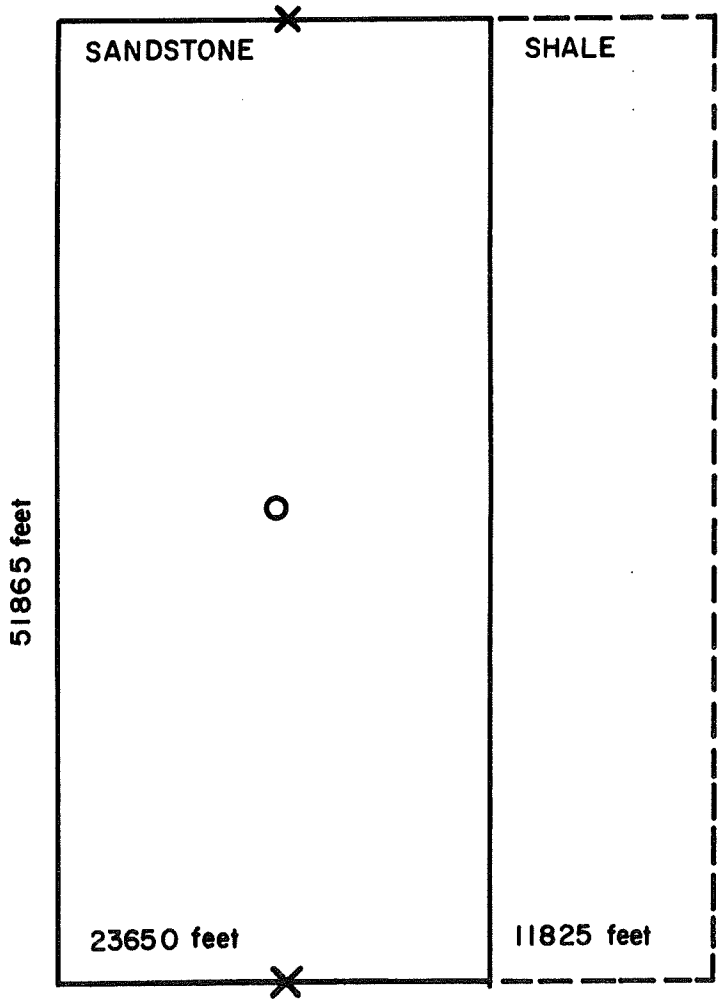

Figure 1

Areal View of the Hypothetical
Bounded Reservoir

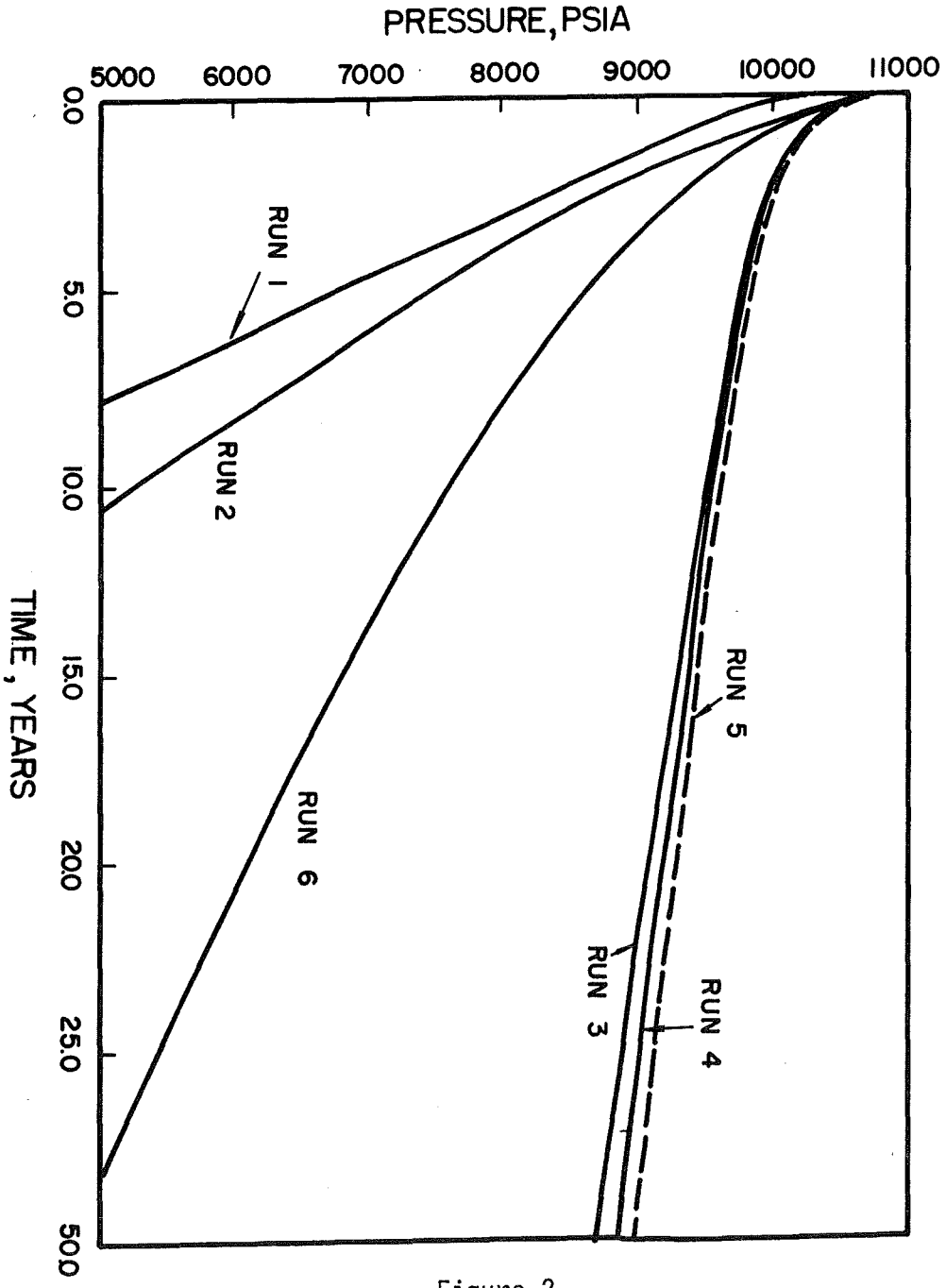

Figure 2

Effects of Solution Gas, Compaction, Shale water Influx and Reinjection on the Well Block Pressure History

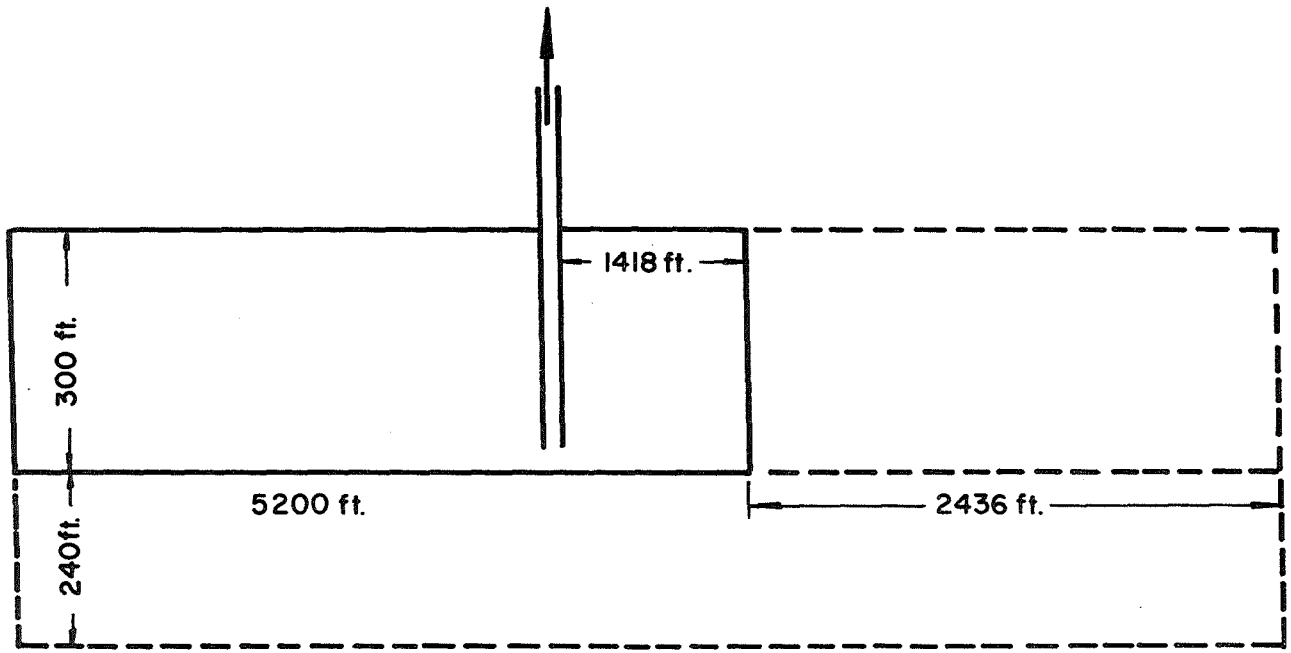

Figure 3

Side View of Cross-sectional
Reservoir with Adjacent and
Underlying Shales

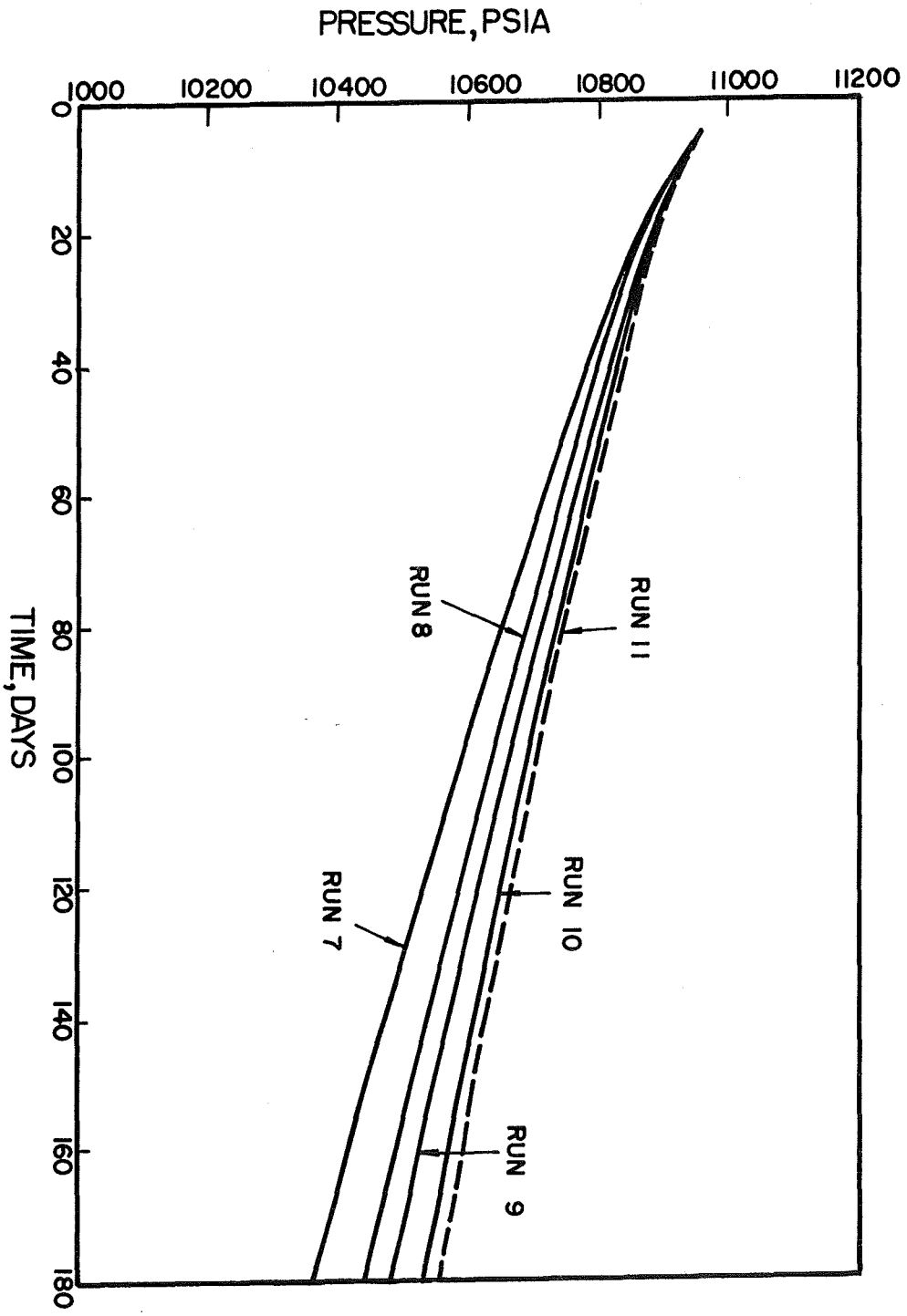

Figure 4

Effects of Shale Water Influx
on Production Sink Pressure
History

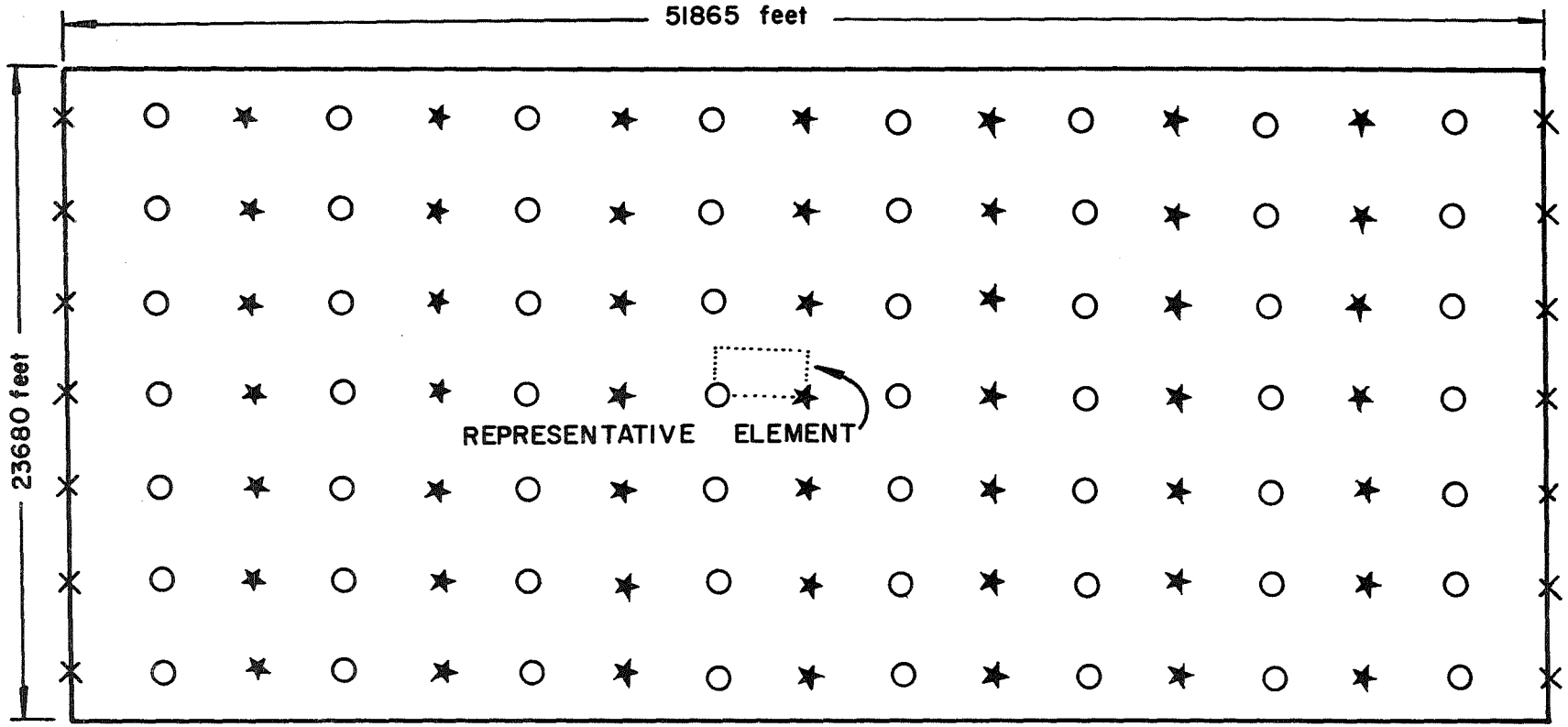

Figure 5

Areal View of Reservoir Showing
Locations of Wells

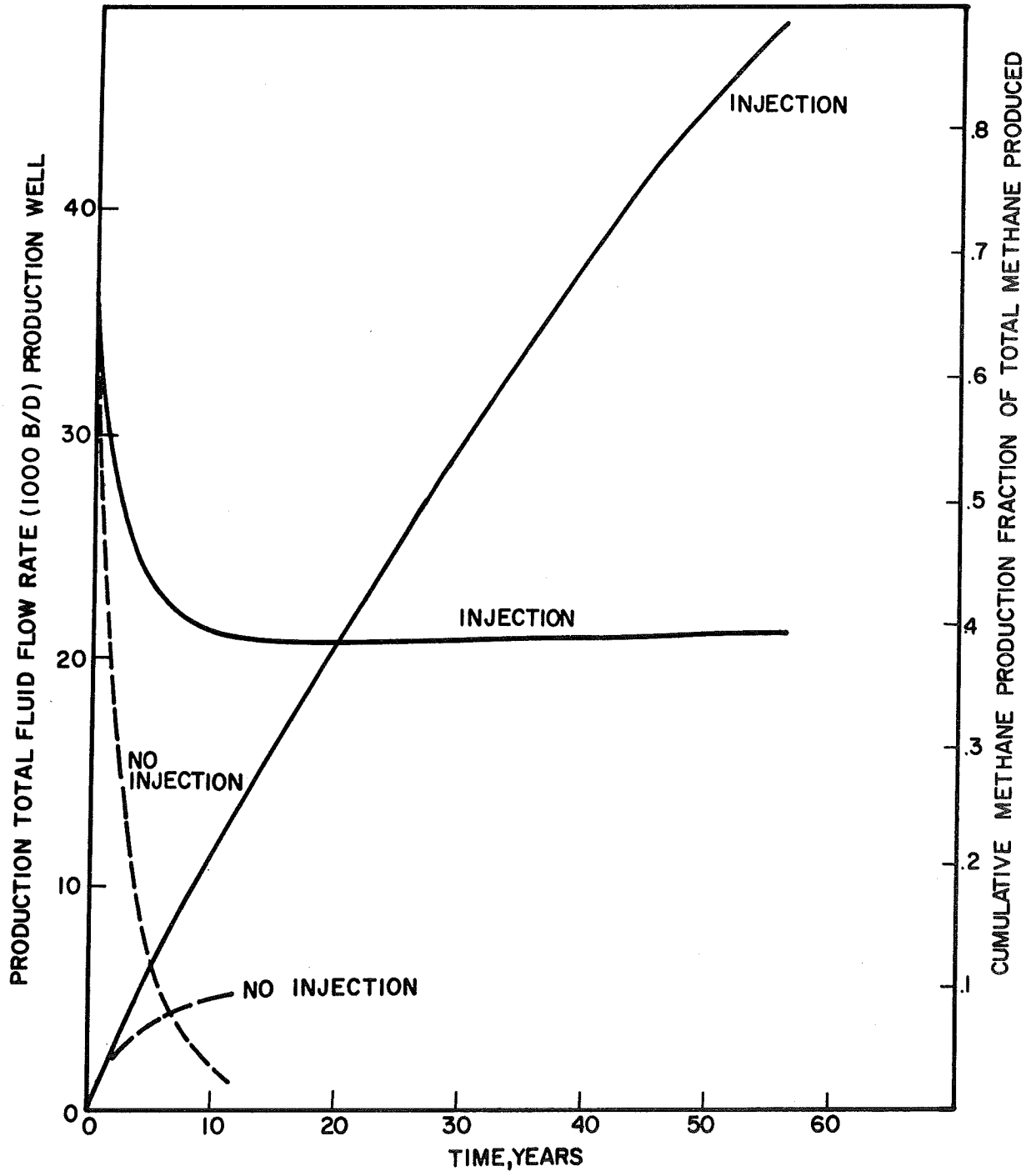

Figure 6

Per Well Production Rate and Cumulative Methane Production Histories of Production Alternatives

TABLE 1

RESERVOIR ROCK PROPERTIES USED FOR EXAMPLE CALCULATIONS

Rock grain density (ρ_{rm})	= 164.4 lbm/cu ft
Heat capacity of rock matrix (C_{vs})	= 0.826 Btu/lb^{o}F
Rock grain thermal conductivity ($\dot{\kappa}_{rm}$)	= 1.566 x 10^{-10} Btu/hr.ft^{o}F
Initial porosity (ϕ_o)	= 0.216
Initial absolute permeability (k_o)	= 18 md
Rock coefficient of linear thermal expansion (η)	= 0
Rock grain coefficient of linear thermal expansion (η_s)	= 0